

A SEARCH FOR VERY HIGH ENERGY GAMMA-RAY EMISSION FROM SCORPIUS X-1 WITH THE MAGIC TELESCOPES

J. ALEKSIĆ¹, E. A. ALVAREZ², L. A. ANTONELLI³, P. ANTORANZ⁴, M. ASENSIO², M. BACKES⁵, J. A. BARRIO², D. BASTIERI⁶, J. BECERRA GONZÁLEZ^{7,8}, W. BEDNAREK⁹, A. BERDYUGIN¹⁰, K. BERGER^{7,8}, E. BERNARDINI¹¹, A. BILAND¹², O. BLANCH¹, R. K. BOCK¹³, A. BOLLER¹², G. BONNOLI³, P. BORDAS¹⁵, D. BORLA TRIDON¹³, V. BOSCH-RAMON¹⁵, I. BRAUN¹², T. BRETZ^{14,26}, A. CAÑELLAS¹⁵, E. CARMONA¹³, A. CAROSI³, P. COLIN¹³, E. COLOMBO⁷, J. L. CONTRERAS², J. CORTINA¹, L. COSSIO¹⁶, S. COVINO³, F. DAZZI^{16,27}, A. DE ANGELIS¹⁶, E. DE CEA DEL POZO¹⁷, B. DE LOTTO¹⁶, C. DELGADO MENDEZ^{7,28}, A. DIAGO ORTEGA^{7,8}, M. DOERT⁵, A. DOMÍNGUEZ¹⁸, D. DOMINIS PRESTER¹⁹, D. DORNER¹², M. DORO²⁰, D. ELSAESSER¹⁴, D. FERENC¹⁹, M. V. FONSECA², L. FONT²⁰, C. FRUCK¹³, R. J. GARCÍA LÓPEZ^{7,8}, M. GARCZARCYK⁷, D. GARRIDO²⁰, G. GIAVITTO¹, N. GODINOVIĆ¹⁹, D. HADASCH¹⁷, D. HÄFNER¹³, A. HERRERO^{7,8}, D. HILDEBRAND¹², D. HÖHNE-MÖNCH¹⁴, J. HOSE¹³, D. HRUPEC¹⁹, B. HUBER¹², T. JOGLER¹³, S. KLEPNER¹, T. KRÄHENBÜHL¹², J. KRAUSE¹³, A. LA BARBERA³, D. LELAS¹⁹, E. LEONARDO⁴, E. LINDFORS¹⁰, S. LOMBARDI⁶, M. LÓPEZ², E. LORENZ^{12,13}, M. MAKARIEV²¹, G. MANEVA²¹, N. MANKUZHIYIL¹⁶, K. MANNHEIM¹⁴, L. MARASCHI³, M. MARIOTTI⁶, M. MARTÍNEZ¹, D. MAZIN^{1,13}, M. MEUCCI⁴, J. M. MIRANDA⁴, R. MIRZOYAN¹³, H. MIYAMOTO¹³, J. MOLDÓN¹⁵, A. MORALEJO¹, P. MUNAR-ADROVER¹⁵, D. NIETO², K. NILSSON^{10,29}, R. ORITO¹³, I. OYA², D. PANEQUE¹³, R. PAOLETTI⁴, S. PARDO², J. M. PAREDES¹⁵, S. PARTINI⁴, M. PASANEN¹⁰, F. PAUSS¹², M. A. PEREZ-TORRES¹, M. PERSIC^{16,22}, L. PERUZZO⁶, M. PILIA²³, J. POCHON⁷, F. PRADA¹⁸, P. G. PRADA MORONI²⁴, E. PRANDINI⁶, I. PULJAK¹⁹, I. REICHARDT¹, R. REINTHAL¹⁰, W. RHODE⁵, M. RIBÓ¹⁵, J. RICO^{25,1}, S. RÜGAMER¹⁴, A. SAGGION⁶, K. SAITO¹³, T. Y. SAITO¹³, M. SALVATI³, K. SATALECKA¹¹, V. SCALZOTTO⁶, V. SCAPIN², C. SCHULTZ⁶, T. SCHWEIZER¹³, M. SHAYDUK¹³, S. N. SHORE²⁴, A. SILLANPÄÄ¹⁰, J. SITAREK⁹, D. SOB CZYNSKA⁹, F. SPANIER¹⁴, S. SPIRO³, A. STAMERRA⁴, B. STEINKE¹³, J. STORZ¹⁴, N. STRAH³, T. SURIĆ¹⁹, L. TAKALO¹⁰, H. TAKAMI¹³, F. TAVECCHIO³, P. TEMNIKOV²¹, T. TERZIĆ¹⁹, D. TESCARO²⁴, M. TESHIMA¹³, M. THOM⁵, O. TIBOLLA¹⁴, D. F. TORRES^{25,17}, A. TREVES²³, H. VANKOV²¹, P. VOGLER¹², R. M. WAGNER¹³, Q. WEITZEL¹², V. ZABALZA^{15,*}, F. ZANDANEL¹⁸, R. ZANIN^{1,*},

¹ IFAE, Edifici Cn., Campus UAB, E-08193 Bellaterra, Spain

² Universidad Complutense, E-28040 Madrid, Spain

³ INAF National Institute for Astrophysics, I-00136 Rome, Italy

⁴ Università di Siena, and INFN Pisa, I-53100 Siena, Italy

⁵ Technische Universität Dortmund, D-44221 Dortmund, Germany

⁶ Università di Padova and INFN, I-35131 Padova, Italy

⁷ Inst. de Astrofísica de Canarias, E-38200 La Laguna, Tenerife, Spain

⁸ Depto. de Astrofísica, Universidad de La Laguna, E-38206 La Laguna, Spain

⁹ University of Łódź, PL-90236 Lodz, Poland

¹⁰ Tuorla Observatory, University of Turku, FI-21500 Piikkiö, Finland

¹¹ Deutsches Elektronen-Synchrotron (DESY), D-15738 Zeuthen, Germany

¹² ETH Zurich, CH-8093 Switzerland

¹³ Max-Planck-Institut für Physik, D-80805 München, Germany

¹⁴ Universität Würzburg, D-97074 Würzburg, Germany

¹⁵ Universitat de Barcelona (ICC/IEEC), E-08028 Barcelona, Spain

¹⁶ Università di Udine, and INFN Trieste, I-33100 Udine, Italy

¹⁷ Institut de Ciències de l'Espai (IEEC-CSIC), E-08193 Bellaterra, Spain

¹⁸ Inst. de Astrofísica de Andalucía (CSIC), E-18080 Granada, Spain

¹⁹ Croatian MAGIC Consortium, Institute R. Boskovic, University of Rijeka and University of Split, HR-10000 Zagreb, Croatia

²⁰ Universitat Autònoma de Barcelona, E-08193 Bellaterra, Spain

²¹ Inst. for Nucl. Research and Nucl. Energy, BG-1784 Sofia, Bulgaria

²² INAF/Osservatorio Astronomico and INFN, I-34143 Trieste, Italy

²³ Università dell'Insubria, Como, I-22100 Como, Italy

²⁴ Università di Pisa, and INFN Pisa, I-56126 Pisa, Italy

²⁵ ICREA, E-08010 Barcelona, Spain

²⁶ now at: Ecole polytechnique fédérale de Lausanne (EPFL), Lausanne, Switzerland

²⁷ supported by INFN Padova

²⁸ now at: Centro de Investigaciones Energéticas, Medioambientales y Tecnológicas (CIEMAT), Madrid, Spain

²⁹ now at: Finnish Centre for Astronomy with ESO (FINCA), University of Turku, Finland and

* Authors to whom correspondence should be addressed: V. Zabalza (vzabalza@am.ub.es) and R. Zanin (roberta@ifae.es)

Submitted 2011 March 29; accepted 2011 May 17; published 2011 June 3

ABSTRACT

The acceleration of particles up to GeV or higher energies in microquasars has been the subject of considerable theoretical and observational efforts in the past few years. Sco X-1 is a microquasar from which evidence of highly energetic particles in the jet has been found when it is in the so-called Horizontal Branch (HB), a state when the radio and hard X-ray fluxes are higher and a powerful relativistic jet is present. Here we present the first very high energy gamma-ray observations of Sco X-1, obtained with the MAGIC telescopes. An analysis of the whole dataset does not yield a significant signal, with 95% CL flux upper limits above 300 GeV at the level of $2.4 \times 10^{-12} \text{ cm}^{-2} \text{ s}^{-1}$. Simultaneous *RXTE* observations were conducted to provide the X-ray state of the source. A selection of the gamma-ray data obtained during the HB based on the X-ray colors did not yield a signal either, with an upper limit of $3.4 \times 10^{-12} \text{ cm}^{-2} \text{ s}^{-1}$. These upper limits place a constraint on the maximum TeV luminosity to non-thermal X-ray luminosity of $L_{\text{VHE}}/L_{\text{ntX}} \lesssim 0.02$, that can be related to a maximum TeV luminosity to jet power ratio of $L_{\text{VHE}}/L_{\text{j}} \lesssim 10^{-3}$. Our upper limits indicate that the underlying high-energy emission physics in Sco X-1 must be inherently different from that of the hitherto detected gamma-ray binaries.

Subject headings: acceleration of particles — stars: individual (Sco X-1) — gamma rays: stars — X-rays: binaries

1. INTRODUCTION

It has been proposed that particles accelerated in relativistic microquasar ejections could produce detectable gamma-ray emission (Atayan & Aharonian 1999). A confirmation of such predictions may be found in Cygnus X-3, an accreting X-ray binary from which non-thermal emission up to energies above 100 MeV has been clearly detected (Tavani et al. 2009; Abdo et al. 2009). However, an extensive observational campaign in the very high energy (VHE) gamma-ray band yielded no detection (Aleksić et al. 2010a). Another well-known microquasar, GRS 1915+105, was observed at VHE but only upper limits were obtained (Saito et al. 2009; Acero et al. 2009). Finally, MAGIC found evidence (at a post-trial significance level of 4.1σ) for VHE gamma-ray emission from the microquasar Cygnus X-1 (Albert et al. 2007), but this has not yet been confirmed through an independent detection.

On the other hand, there are three binary systems that have been unambiguously detected at TeV energies: LS 5039 (Aharonian et al. 2005b), LSI+61 303 (Albert et al. 2006), and PSR B1259–63 (Aharonian et al. 2005a). However, none of them can be clearly classified as a microquasar. The nature of the compact object in LS 5039 and LSI+61 303 is unknown: although it was originally proposed that they were accreting microquasars (Paredes et al. 2000; Massi et al. 2004), there is growing evidence that they might contain a young non-accreting pulsar (Dubus 2006), as is also the case for PSR B1259–63 (Johnston et al. 1992). A fourth candidate is HESS J0632+057, a galactic plane point-like TeV source with variable radio, X-ray and TeV emission (Skilton et al. 2009, and references therein). Recent observations have resulted in the detection of a 320 ± 5 day X-ray period (Bongiorno et al. 2011), and detection of slightly extended radio emission at milliarcsecond scales (Moldón et al. 2011) similar to that found in all other gamma-ray binaries.

In the case of the microquasar Cygnus X-1, the massive, luminous stellar companion provides an intense target photon field for inverse Compton (IC) scattering. However, this photon field could also absorb the produced gamma-rays through pair production with opacities up to 10 at 1 TeV (Bednarek & Giovannelli 2007). Such strong absorption might not be present in the case of low-mass X-ray binaries (LMXBs), where the companion star has a lower mass and, correspondingly, a lower luminosity. Low-mass systems with persistent accretion and powerful relativistic jets could produce TeV emission via synchrotron self-Compton (SSC), and would be good candidates to be detected at these energies given their continuous activity and the lack of severe absorption. However, external IC cannot be fully discarded in LMXBs given strong accretion disk emission (Bosch-Ramon et al. 2006) or X-ray-enhanced radiation from the stellar companion, which would also increase the TeV opacities (Bednarek & Pabich 2010).

The Z sources are a class of LMXBs that contain a low magnetic field neutron star accreting close to the Eddington limit. Their X-ray intensities and colors change on timescales of hours, and their paths in a hard color versus soft color diagram follow roughly Z-shaped tracks (Hasinger & van der Klis 1989). Along this track the sources change between different spectral states known as Horizontal Branch (HB), Normal Branch (NB), and Flaring Branch (FB). A traditional

interpretation of these different X-ray states is a variation in the mass accretion rate. Recent evidence, however, points towards constant mass accretion rate along the Z track (Homan et al. 2010), whereas different mass accretion rates would give rise to the different LMXB subclasses. Since most LMXBs have almost circular orbits, the X-ray states are not expected to have an orbital dependence. Even though known as a Z track, with the HB being the upper-left horizontal part of the track, in some sources the tracks may be more accurately described by a double banana shape, with the upper banana being the part corresponding to the HB/NB states and the lower banana corresponding to the NB/FB states (Hasinger & van der Klis 1989). Radio emission and hard X-ray power-law tails, strong evidence of particle acceleration up to very high energies, have been only detected while the sources are in the HB (Hjellming et al. 1990; Di Salvo et al. 2006).

Sco X-1, located at 2.8 ± 0.3 kpc, is a prototype Z-type LMXB with an orbital period of 0.787 days that contains a low magnetic field neutron star and a $0.4 M_{\odot}$ M star. The circular binary orbit has an inclination of 44° and a separation of $\sim 1.5 \times 10^{11}$ cm (see Fomalont et al. 2001, Steeghs & Casares 2002, and references therein). Accretion takes place via Roche lobe overflow. The source displays a double banana track in color-color diagrams (CD) and covers the whole track in a few tens of hours, spending roughly half of the time in the HB. Spectral fits at hard X-rays reveal a non-thermal power law with higher fluxes during the HB, reaching values in the range 10^{-10} – 10^{-9} erg cm $^{-2}$ s $^{-1}$, and no high-energy cutoff (Di Salvo et al. 2006; D’Aí et al. 2007). Moreover, twin relativistic radio lobes moving at $\sim 0.5c$ from the central source have been detected, while successive flaring of the core and lobes reveals the action of an unseen, highly relativistic flow with a speed above $0.95c$ (Fomalont et al. 2001). All these results clearly indicate the injection of highly energetic particles when the source is in the HB, and suggest that the IC (likely SSC) process could be at work when a powerful jet is present in this spectral state. The IC process could generate VHE emission but, to adequately assess its origin, simultaneous X-ray observations are required to monitor the source X-ray state. Sco X-1 was claimed to be a source of TeV and PeV gamma-rays (Brazier et al. 1990; Tonwar et al. 1991), but the low significance and lack of later confirmation shed doubts on this evidence.

In 2010 May we carried out a simultaneous observation campaign with the Cherenkov VHE gamma-ray telescopes MAGIC and the X-ray observatory *RXTE*. Here we present the results of the first VHE observations of Sco X-1 for selected X-ray states, focusing on the HB state, where evidence for relativistic particles in the jet has already been found.

2. OBSERVATIONS AND DATA ANALYSIS

2.1. MAGIC

MAGIC consists of two 17 m diameter Imaging Atmospheric Cherenkov Telescopes located at the Roque de los Muchachos Observatory on the Canary Island of La Palma (28° N, 18° W, 2200 m). It became a stereoscopic system in autumn 2009. Since then, the instrument sensitivity almost doubled with respect to the one of the stand-alone telescope operation mode, and currently it yields, at low zenith angles, 5σ significance detections above 250 GeV of fluxes as low

Table 1
Log of the VHE Observations.

Date ^a (MJD)	Orbital Phase	Eff. Time (hr)	X-ray State	UL (> 300 GeV) ^b (cm ⁻² s ⁻¹)	C.U.
55331.09	0.26–0.38	1.28	NB/FB	7.9×10^{-12}	6.4%
55332.11	0.58–0.64	0.48	HB	5.2×10^{-12}	4.2%
55333.07	0.77–0.86	1.65	NB/FB	3.5×10^{-12}	2.8%
55334.06	0.03–0.12	1.37	HB	5.1×10^{-12}	4.1%
55335.05	0.25–0.39	1.73	HB	5.3×10^{-12}	4.3%
55336.06	0.52–0.66	1.24	NB	2.0×10^{-12}	1.6%

^a The central MJD of each observation is quoted.

^b Upper limits at 95% confidence level.

as 0.8% of the Crab Nebula flux in 50 hr (Colin et al. 2009; Aleksić et al. 2011).

MAGIC observed Scorpius X-1 at high zenith angles, between 43° and 50°, for a total amount of 7.75 hr during six consecutive nights in 2010 May. Table 1 shows the detailed observation log.

Data analysis was performed using the standard MAGIC analysis software. Each telescope records only the events selected by the hardware stereo trigger. The obtained images are reconstructed, and parameterized (Aliu et al. 2009). The two images from the same stereo event are combined, and the shower direction is determined as the intersection of the corresponding single-telescope directions (Aleksić et al. 2010b). The background rejection relies on the definition of a global variable, called *hadronness*, which is computed by means of a Random Forest algorithm (Albert et al. 2008a). The γ -ray signal is estimated through the distribution of the squared angular distance between the reconstructed and the catalog source position (θ^2). The energy of each event is estimated by using look-up tables created from Monte Carlo simulated γ -ray events. The sensitivity of this high-zenith-angle analysis is 1.1% of the Crab Nebula flux for energies above 300 GeV in 50 hr.

For the case of non-detections, we computed flux upper limits using the method of Rolke et al. (2005) including a 30% systematic uncertainty. The source spectrum was assumed to be a power law with a photon index of $\Gamma = 3$. This photon index was taken to account for the possibility that the spectrum of Sco X-1 is steeper than the Crab Nebula one, as would be the case for some of the plausible emission scenarios (see Section 4). However, it must be noted that a 30% change in the assumed photon index yields a variation of less than 1% in the flux upper limits. The integral upper limits apply to the photon fluxes from Sco X-1 at energies above 300 GeV and correspond to a confidence level of 95%. A calculation of energy flux upper limits from the differential photon flux upper limits yields a variation of $\sim 1.5\%$ when considering a 30% change in the assumed photon index.

2.2. X-rays

Sco X-1 was observed with *RXTE* simultaneously with the MAGIC VHE gamma-ray observations. To study the source X-ray spectral state, we analyzed the data from the Proportional Counter Array instrument (PCA), which is sensitive in the range 2–60 keV. To calculate the CD of Sco X-1 we extracted soft color and hard color lightcurves in 64 s bins, where the soft color is defined as the ratio between the count rate in the energy bands [4.08–6.18 keV]/[1.94–4.05 keV] and the hard color is the ratio [8.32–16.26 keV]/[6.18–8.32 keV]. These

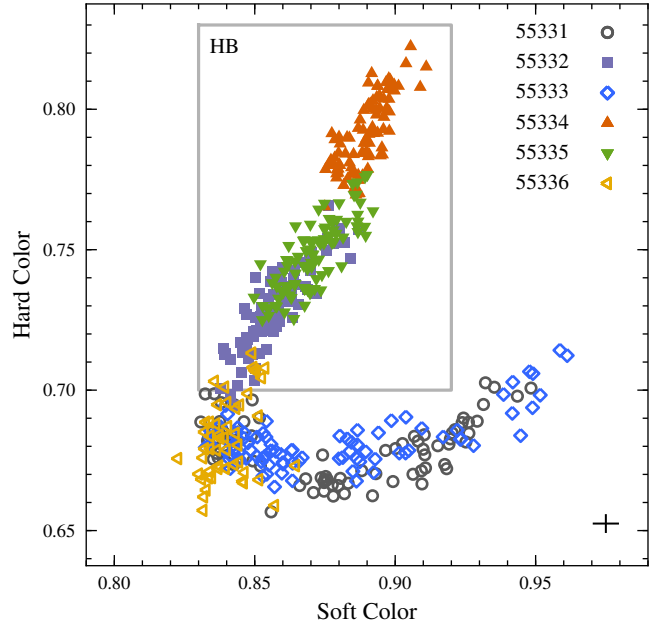


Figure 1. X-ray color-color diagram of Sco X-1 from the *RXTE*/PCA data obtained during the simultaneous MAGIC campaign. See the text for a definition of the Hard and Soft colors. The typical relative error of each measurement is around 0.5% and is shown by a black cross at the bottom-right corner. The HB selection range is indicated by the gray box. The different symbols and colors indicate each of the different observation days, labeled in MJD. The filled symbols indicate days selected as HB and empty symbols days selected as NB or FB.

energy ranges are equivalent to those used in previous studies of the source (e.g., D’Aí et al. 2007). The resulting CD for the whole observational campaign is shown in Figure 1, where it can be seen that the source practically covered the full double banana-shaped track during the observations. We selected the top part of the upper banana of the CD (indicated by a gray box in Figure 1) as corresponding to the HB. This selection is supported by previous observations of Sco X-1 with *RXTE*, where periods with similar CD selections were found to show the hard X-ray power-law component characteristic of the HB state (Di Salvo et al. 2006; D’Aí et al. 2007).

3. RESULTS

A night-by-night analysis of the X-ray spectral states of Sco X-1 showed that the source did not move extensively along the Z track during any of the individual observation nights, as can be seen in Figure 1. During three of the six VHE observations the source was in the HB (MJD 55332, 55334 and 55335), as indicated in the observation log of Table 1.

The total significance (following the definition of Li & Ma 1983) of the gamma-ray signal coming from Sco X-1 for the complete data set of MAGIC observations, which amounts to 7.75 hr of effective time, is $S = 0.52\sigma$. For the complete dataset, the computed flux upper limit is $2.4 \times 10^{-12} \text{ cm}^{-2} \text{ s}^{-1}$ above 300 GeV. The simultaneous X-ray observations allowed us to select the VHE data corresponding to each X-ray state. We performed a signal search for those periods when the source was in the HB, but no significant excess was found, with a flux upper limit of $3.4 \times 10^{-12} \text{ cm}^{-2} \text{ s}^{-1}$ above 300 GeV. A search for a signal in the rest of the data set, when the source was in NB and FB states, did not produce a positive result either. A summary of the X-ray-state selected results for the VHE data is shown in Table 2.

Additionally, a night-by-night analysis was performed.

Table 2
Integral Upper Limits for Selected X-ray States

X-ray State	Effective Time (hr)	Significance σ	UL (> 300 GeV) ^a ($\text{cm}^{-2} \text{s}^{-1}$)	C.U.
All	7.75	0.52	2.4×10^{-12}	1.9%
HB	3.58	0.72	3.4×10^{-12}	2.7%
NB/FB	4.17	0.08	2.8×10^{-12}	2.3%

^a Upper limits at 95% confidence level.

In none of the six observations was a significant signal found; the corresponding flux upper limits are between $2.0 \times 10^{-12} \text{ cm}^{-2} \text{ s}^{-1}$ and $7.9 \times 10^{-12} \text{ cm}^{-2} \text{ s}^{-1}$, as shown in Table 1.

In Figure 2, we show the differential flux upper limits computed for the HB state and the whole data set to serve as a constraint for future theoretical modeling of the VHE emission of the source. Differential photon flux upper limits may also be used to obtain energy flux upper limits. Taking $\Gamma = 3$, we obtain integral energy flux upper limits of 3.3, 5.6, and $5.4 \times 10^{-12} \text{ erg cm}^{-2} \text{ s}^{-1}$ above 300 GeV for the whole data set, the HB data and the NB/FB data, respectively.

4. DISCUSSION

To put in context the MAGIC results and understand the potentialities of Sco X-1 to produce VHE emission, in this section we discuss some of the possible emission scenarios. We consider the energy budget available from the relativistic jet and the processes that could give rise to VHE emission either at its base or further away from the compact object. Finally, we compare Sco X-1 with other microquasars and the detected gamma-ray binaries, and conclude with a brief summary.

The emitter properties will be mostly constrained by the jet power, which dictates the maximum energy budget available, and the emitter size and location. The jet luminosity (L_j) can be fixed assuming that the power-law hard X-rays come from the jet, and assuming an X-ray luminosity to total jet power ratio of 0.01–0.1. Given that the power-law luminosity is $L_{\text{ntX}} \sim 10^{35} - 10^{36} \text{ erg s}^{-1}$, a value of $L_j \sim 10^{37} \text{ erg s}^{-1}$ seems reasonable, and is also high enough to account for the radio emission from the source (Fomalont et al. 2001). The VHE luminosity upper limits in the HB show that Sco X-1 has a maximum VHE luminosity to jet power ratio of $L_{\text{VHE}}/L_j \lesssim 10^{-3}$. This value is slightly below the ratio inferred for the Cygnus X-1 flare (Albert et al. 2007), and similar to the upper limit of Cygnus X-3 (Aleksić et al. 2010a), but an order of magnitude above the upper limit for GRS 1915+105 (Acero et al. 2009). However, given the transient nature of these sources, the orbital coverage and total length of the observational campaign play a role in their eventual detection. We note that the campaign presented here is relatively short and does not provide a complete orbital coverage so it does not rule out the possibility of VHE flares from Sco X-1.

Assuming that the jet of Sco X-1 can indeed accelerate particles efficiently, there are several possible reasons to explain the MAGIC non-detection. We will begin by considering the possibility that particles are accelerated in the jet base and the power-law hard X-rays are emitted there. At this location, it may be difficult to accelerate particles beyond 100 GeV because of strong radiative cooling. The emitted spectrum is likely to be very soft because of the dominant synchrotron cooling and IC occurring deep in the Klein-Nishina regime. In addition, the radiation from 10 GeV to 1 TeV would likely be absorbed through pair creation by the intense radiation field

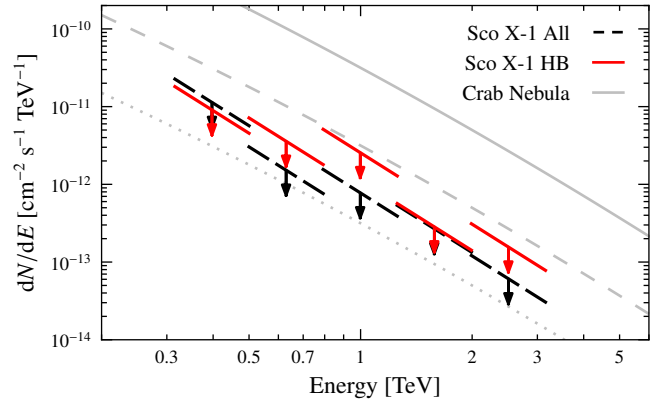


Figure 2. Differential upper limits for all the observations (black, dashed) and for the days in the HB (red). The slope of the bar indicates the assumed power-law photon index in the calculation of the upper limit. The Crab Nebula spectrum (Albert et al. 2008b) is shown for comparison, as well as its 10% (dashed) and 1% (dotted) fractions.

from the accretion disc. At this location, even lower energy GeV photons would be absorbed. However, if the magnetic field is low enough and electromagnetic cascading (e.g., Aharonian & Vardanian 1985) is efficient, absorption at the jet base owing to the disc photon field might not be so relevant. Another source of absorption is the stellar photon field, enhanced through accretion X-ray irradiance of the stellar surface, and could be optically thick for VHE gamma-rays in some orbital phases. Note however that MAGIC has not detected the source even for those phases in which this source of gamma-ray absorption should be negligible: on MJD 55334 the source was $\phi=0.03-0.12$, for which the expected gamma-ray opacity is $\tau \sim 0.1$ (Bednarek & Pabich 2010). The combined effect of a steep gamma-ray spectrum and pair creation absorption would diminish the chances of a VHE detection, particularly for an observation at high zenith angles and correspondingly high energy threshold as presented here.

On the other hand, radiation at VHE produced farther from the compact object, at distances above 10^8 cm , could be eventually detected. The SSC channel, efficient for intermediate values of the magnetic field, would yield a less steep spectrum and may occur in regions where the emitter and the environment are optically thin to VHE photons. IC with the X-ray enhanced stellar photon field could also yield significant and less steep VHE radiation and would be most efficient for optical depths of order of unity. According to the calculations of Bednarek & Pabich (2010), this would take place around orbital phases close to 0.3 and 0.7, but we did not detect such emission on MJD 55335 at orbital phases 0.25–0.39. At these high altitudes in the jet, GeV photons could easily escape the system and produce detectable high-energy gamma-ray emission. The eventual detection of Sco X-1 by *Fermi* or *AGILE*, plus a non-detection with low-enough upper limits at VHE, would likely favor the scenario where gamma-ray radiation is emitted from a location far away from the neutron star but with a spectrum too steep for a VHE detection. Synchrotron cooling dominance could explain the steep spectrum and would mean that the power-law hard X-rays have a synchrotron origin. We note that the energy flux of an SSC/IC spectral component peaking at 1 GeV, with $\Gamma = 3$ at higher energies and consistent with our upper-limit during the HB, would only represent, at most, 0.8% of the Eddington luminosity for the neutron star.

For leptonic emission scenarios, such as the SSC and exter-

nal IC described above, it can be assumed that X-ray emission has a synchrotron origin and VHE gamma-rays have an IC origin. The VHE to non-thermal X-ray luminosity ratio is then a sensitive indicator of the importance of synchrotron cooling and ultimately of the magnetic field of the emitter. For the case of Sco X-1, and considering only the hard X-ray power law as non-thermal X-ray emission, this ratio has a maximum value of $L_{\text{VHE}}/L_{\text{ntX}} \lesssim 0.02$ for the HB. On the hitherto detected gamma-ray loud X-ray binaries this ratio is much higher. For the case of LSI +61 303, for example, the VHE to X-ray ratio is between 0.5 and 1 during the X-ray and VHE peak at phases $\phi = 0.6\text{--}0.7$ (Anderhub et al. 2009). Even considering the average fluxes for the full simultaneous campaign during 60% of an orbit the ratio is 0.26. In both cases, the VHE to X-ray luminosity ratio is higher than the value we obtained for Sco X-1 by more than an order of magnitude. However, as mentioned above for the comparison with other microquasars, the short total length of the observational campaign presented here prevents us from making absolute comparisons because of the possible transient nature of the source. On the other hand, if there is no such flaring behavior, the difference in the VHE to X-ray luminosity ratios indicates that the underlying physics is significantly different than for LSI +61 303 or LS 5039.

In conclusion, our results place the first upper limits on the VHE gamma-ray emission from Sco X-1 in all of the X-ray states of the source. If Sco X-1 is indeed capable of producing TeV emission, either a longer observational campaign, with better orbital coverage (to probe phase-dependent effects such as absorption, cascading, etc.), or an instrument with a significant increase in sensitivity, such as the future Cherenkov Telescope Array (CTA), might be required to detect it. Our upper limits also indicate that the underlying VHE emission physics may be inherently different in the case of Sco X-1 and the detected gamma-ray binaries.

This research project has made use of data collected by NASA's *RXTE*. We thank the *RXTE* scheduling team for their help in coordinating the simultaneous observations. We also thank the Instituto de Astrofísica de Canarias for the excellent working conditions at the Observatorio del Roque de los Muchachos in La Palma. The support of the German BMBF and MPG, the Italian INFN, the Swiss National Fund SNF, and the Spanish MICINN is gratefully acknowledged. This work was also supported by the Marie Curie program, by the CPAN CSD2007-00042 and MultiDark CSD2009-00064 projects of the Spanish Consolider-Ingenio 2010 programme, by grant DO02-353 of the Bulgarian NSF, by grant 127740

of the Academy of Finland, by the YIP of the Helmholtz Gemeinschaft, by the DFG Cluster of Excellence ‘‘Origin and Structure of the Universe’’, and by the Polish MNiSzw grant 745/N-HESS-MAGIC/2010/0.

Facilities: RXTE (PCA), MAGIC

REFERENCES

- Abdo, A. A., et al. 2009, *Science*, 326, 1512
 Acero, F., et al. 2009, *A&A*, 508, 1135
 Aharonian, F., et al. 2005a, *A&A*, 442, 1
 —. 2005b, *Science*, 309, 746
 Aharonian, F. A., & Vardanian, V. V. 1985, *Ap&SS*, 115, 31
 Albert, J., et al. 2006, *Science*, 312, 1771
 —. 2007, *ApJ*, 665, L51
 —. 2008a, *Nucl. Instrum. and Methods Phys. Res. A*, 588, 424
 —. 2008b, *ApJ*, 674, 1037
 Aleksić, J., et al. 2010a, *ApJ*, 721, 843
 —. 2010b, *A&A*, 524, A77
 —. 2011, in preparation
 Aliu, E., et al. 2009, *Astropart. Phys.*, 30, 293
 Anderhub, H., et al. 2009, *ApJ*, 706, L27
 Atayan, A. M., & Aharonian, F. A. 1999, *MNRAS*, 302, 253
 Bednarek, W., & Giovannelli, F. 2007, *A&A*, 464, 437
 Bednarek, W., & Pabich, J. 2010, *A&A*, 514, A61+
 Bongiorno, S., Falcone, A., Stroh, M., Holder, J., Skilton, J., Hinton, J., Gehrels, N., & Grube, J. 2011, *ApJL*, in press (arXiv:1104.4519)
 Bosch-Ramon, V., Romero, G. E., & Paredes, J. M. 2006, *A&A*, 447, 263
 Brazier, K. T. S., et al. 1990, *A&A*, 232, 383
 Colin, P., et al. 2009, in *Proc. 31st ICRC (Łódź)*, 342 (arXiv:0907.0960)
 D’Aí, A., Życki, P., Di Salvo, T., Iaria, R., Lavagetto, G., & Robba, N. R. 2007, *ApJ*, 667, 411
 Di Salvo, T., et al. 2006, *ApJ*, 649, L91
 Dubus, G. 2006, *A&A*, 456, 801
 Fomalont, E. B., Geldzahler, B. J., & Bradshaw, C. F. 2001, *ApJ*, 558, 283
 Hasinger, G., & van der Klis, M. 1989, *A&A*, 225, 79
 Hjellming, R. M., et al. 1990, *ApJ*, 365, 681
 Homan, J., et al. 2010, *ApJ*, 719, 201
 Johnston, S., Manchester, R. N., Lyne, A. G., Bailes, M., Kaspi, V. M., Qiao, G., & D’Amico, N. 1992, *ApJ*, 387, L37
 Li, T., & Ma, Y. 1983, *ApJ*, 272, 317
 Massi, M., Ribó, M., Paredes, J. M., Garrington, S. T., Peracaula, M., & Martí, J. 2004, *A&A*, 414, L1
 Moldón, J., Ribó, M., & Paredes, J. 2011, *ATel*, 3180
 Paredes, J. M., Martí, J., Ribó, M., & Massi, M. 2000, *Science*, 288, 2340
 Rolke, W. A., López, A. M., & Conrad, J. 2005, *Nucl. Instrum. and Methods Phys. Res. A*, 551, 493
 Saito, T. Y., et al. 2009, in *Proc. 31st ICRC (Łódź)*, 1233 (arXiv:0907.1017)
 Skilton, J. L., et al. 2009, *MNRAS*, 399, 317
 Steeghs, D., & Casares, J. 2002, *ApJ*, 568, 273
 Tavani, M., et al. 2009, *Nature*, 462, 620
 Tonwar, S. C., Gopalakrishnan, N. V., Gupta, S. K., Rajeev, M. R., Sreekantan, B. V., & Srivatsan, R. 1991, *Phys. Rev. Lett.*, 67, 2248